

Structure-Based Macrocyclization Yields Hepatitis C Virus NS5B Inhibitors with Improved Binding Affinities and Pharmacokinetic Properties

Maxwell D. Cummings,* Tse-I Lin, Lili Hu, Abdellah Tahri, David McGowan, Katie Amssoms, Stefaan Last, Benoit Devogelaere, Marie-Claude Rouan, Leen Vijgen, Jan Martin Berke, Pascale Dehertogh, Els Fransen, Erna Cleiren, Liesbet van der Helm, Gregory Fanning, Kristof Van Emelen, Origène Nyanguile, Kenny Simmen, Pierre Raboisson, and Sandrine Vendeville*

Macrocyclization is one molecular design strategy that can be used to improve the drug-related characteristics of small molecules and peptides,^[1–4] and thus may provide a route to a less restrictive “drug-likeness space”. Structure-based design is typically focused on the optimization of a chemical series to increase affinity toward a target protein: modification to gain additional binding contacts and rigidification to favor a bio-active conformation are two common strategies. In addition to affinity for the primary target, a 3D structure of a relevant protein–small molecule complex can be used to guide the optimization of other pharmaceutical properties. Substituent positions that project away from the binding site may be chemically exploited to alter one or more PK- or ADME-related properties (e.g. “solubilizing groups”) while having minimal effect on the therapeutically relevant binding interaction (PK = pharmacokinetics; ADME = absorption, distribution, metabolism, and excretion). Pursuing a design strategy based on publicly available 3D structures, we combined rigidification and the introduction of a PK-enhancing group in a single modification by forming a macrocycle between two solvent-exposed substituent positions of a small-molecule inhibitor of an essential viral enzyme. This approach

yielded new inhibitors with improved PK properties as well as increased enzyme affinities and antiviral activities, while appearing less drug-like according to standard calculated criteria.

A series of indole-based inhibitors is known to bind to a cryptic site of the thumb domain of the NS5B RNA polymerase (NS5B) of hepatitis C virus (HCV) remote from the active site,^[5–7] and crystal structures of three early indole inhibitors bound to this site are available from the protein data bank (PDB) (Figure 1).^[5,6] In these structures the cyclohexyl ring and one edge of the phenyl and indole rings project into the hydrophobic binding pocket, while the more polar indole N-substituents and the carboxylate are largely solvent-exposed. The exposed carboxylate forms a salt bridge with Arg503 at the edge of the binding pocket, an important binding interaction (Figure 1).^[8]

Several groups have studied the indole series of NS5B inhibitors, exploring bioisosteres of the parent carboxylate (e.g. amide, acylsulfonamide, acylsulfamide) as well as introducing solvent-exposed permeability- and/or PK-enhancing substituents on the indole N.^[6,8–10] Combined with scaffold rigidification, these approaches have yielded new tetracyclic (e.g. 2DXS in Figure 1) and pentacyclic systems with enhanced binding affinities.^[6,7,11] Unfortunately, the resultant compounds have been burdened with pharmaceutically undesirable physico-chemical properties or one or more undesirable structural features. For example, carboxylates were shown to produce potentially toxic or immunogenic acyl glucuronides through a phase-two metabolic pathway,^[12–14] and such acyl glucuronides have been observed with the early leads **4**^[8,15] and **5**^[7] (Figure 2). Furthermore, the permeability/PK-enhancer strategy evolved almost exclusively to zwitterionic molecules possessing a solvent-exposed basic amine,^[7,8,16] a feature that could cause high inter-patient variability in absorption.^[17]

We hypothesized that we could address the PK limitations of the indoles by macrocyclization of the solvent-exposed inhibitor moieties. An initial set of macrocycles was designed and evaluated by molecular modeling and conformational analysis.^[18] Overlay of the three publicly available complex structures indicated that macrocyclization through a tether between the carboxylate and either the indole N or the bridged-phenyl moiety was consistent with the observed


[*] Dr. M. D. Cummings, Dr. T. Lin, L. Hu, Dr. A. Tahri, D. McGowan, Dr. K. Amssoms, S. Last, Dr. B. Devogelaere, M.-C. Rouan, Dr. L. Vijgen, Dr. J. M. Berke, P. Dehertogh, E. Fransen, E. Cleiren, L. van der Helm, Dr. G. Fanning, Dr. K. Van Emelen, Prof. Dr. O. Nyanguile, Dr. K. Simmen, Dr. P. Raboisson, Dr. S. Vendeville

Janssen Infectious Diseases BVBA (formerly Tibotec BVBA)
Turnhoutseweg 30, 2340 Beerse (Belgium)
E-mail: svendev1@its.jnj.com

Dr. M. D. Cummings
Janssen Research & Development
Welsh & McKean Roads, Spring House, PA 19477 (USA)
E-mail: mcummin1@its.jnj.com

Dr. B. Devogelaere
Biocartis NV, Mechelen (Belgium)

Prof. Dr. O. Nyanguile
University of Applied Sciences, Institute of Life Technologies
Rte du Rawyl 47, 1950 Sion 2 (Switzerland)

 Supporting information for this article (full references, protein crystallography, and inhibitor synthesis and characterization) is available on the WWW under <http://dx.doi.org/10.1002/anie.201200110>.

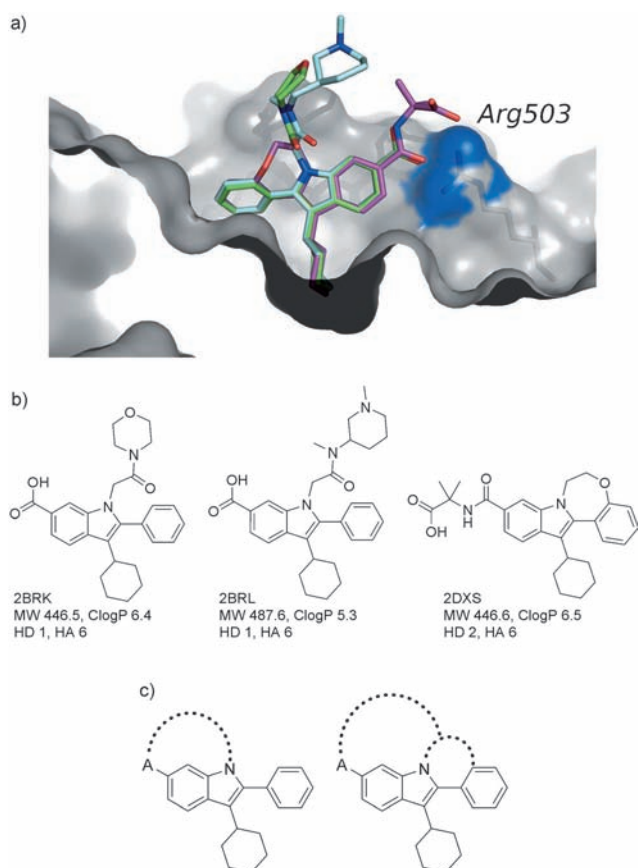


Figure 1. Indole inhibitors of HCV NS5B. a) Overlay of the three early inhibitors with structures available from the PDB (2BRK green color-by-atom, 2BRL cyan color-by-atom, 2DXS magenta color-by-atom), based on superposition of conserved secondary structure elements in the region of the indole binding site. b) Inhibitor chemical structures, PDB ID codes of the complex structures and various properties of the small-molecule inhibitors (MW = molecular weight in g mol^{-1} ; clogP = logarithm of the partition coefficient between *n*-octanol and water; HD = number of hydrogen-bond donors; HA = number of hydrogen-bond acceptors). c) General macrocyclization design schemes.

indole binding mode (Figure 1). Attractively, this approach also maintained the contact with Arg503 while restraining the solvent-exposed inhibitor moieties. Our macrocyclization strategy was initially validated by comparing open and cyclized amide analogues.^[19] Likely carboxylate replacements^[10] were tested in our macrocyclization strategy to optimize the key polar interaction with Arg503.^[19] Previous structural studies investigating the biaryl torsion^[6] and our own explorations^[18] led us to focus on the tetracyclic indole-based system. Subsequent lead optimization focused on the more potent acylsulfamide derivatives combined with the more rigid tetracyclic macrocycle template, exploring macrocycle size, substituents on nitrogens and on the phenyl ring, and the linker between the phenyl and the indole rings.^[18] Our design strategy quickly showed promise, yielding molecules with enhanced binding affinities and improved pharmacokinetic profiles,^[18] and led to the discovery of inhibitors **6** and **7** (see Supporting Information for inhibitor synthesis and characterization), based on a tetracyclic core with two amide

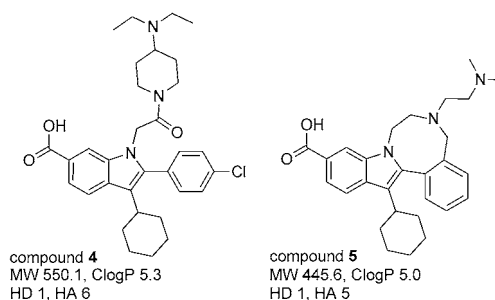


Figure 2. Indole inhibitors **4**^[7,8] and **5**.^[7]

substituents connected by acylsulfamide-containing tethers in a 17- or 16-membered macrocycle, respectively (Figure 3).

We determined the 2.1 Å resolution crystal structure of **7** bound to NS5B.^[20] Bound **7** occupies the expected thumb domain site (Figure 3).^[21] The observed binding mode of the tetracyclic core of the designed macrocyclic inhibitor is fully consistent with the three public structures of non-macrocyclic inhibitor complexes that formed the basis of our structure-based design strategy (Figure 1).^[22] The macrocycle linker is directed away from the protein surface, with the constrained acylsulfamide replacing the carboxylate of previous inhibitors, forming two hydrogen bonds with the guanidine of Arg503, mimicking the contacts observed in previous NS5B-indole complexes (Figure 3).^[5,6]

Previous structural and mechanistic studies indicate a key function for the fingertip Δ 1 loop–thumb domain interaction.^[5,23] Binding of indole inhibitors blocks the fingertip–thumb interaction, inhibiting polymerase activity by, apparently, locking NS5B in an inactive “open” conformation.^[5,23] In past complexes,^[5,6] residues 22–35 of the displaced loop have been disordered. Interestingly, the **7**–NS5B complex reveals new structural information about the binding site, with four of the loop residues (residues 22 and 33–35) disordered in previous structures now resolved; in the new structure residues 33–35 form a helical turn positioned to more fully enclose the methoxyphenyl ring of bound **7** (Figure 3b). The more enclosed binding site and presumably smaller protein conformational change observed for the **7**–NS5B complex may be due to a specific (but weak, given the observed distance) intermolecular hydrogen bond between the macrocycle carbonyl of **7** and His34 (Figure 3c). Such a contact also seems likely for **6**, but is unlikely or impossible for most other reported indole and benzimidazole NS5B inhibitors, assuming a similar binding mode.

Additional binding interactions and/or different conformational adjustments (protein and/or inhibitor) required for binding may explain the higher binding affinities and lower off-rates of macrocycles **6** and **7**, compared to the acyclic predecessor **4** (Table 1). The consequent longer inhibition half-lives of the macrocycles may be relevant to therapeutic efficacy.^[24] Enzymatic and replicon potencies do not fully parallel binding affinities; high protein binding (> 99% in human serum for both macrocycles) rather than limited permeability may account for this discrepancy, and explains the 8- to 9-fold shift in EC_{50} measured under high serum conditions (Table 1). Rather than trying to minimize the

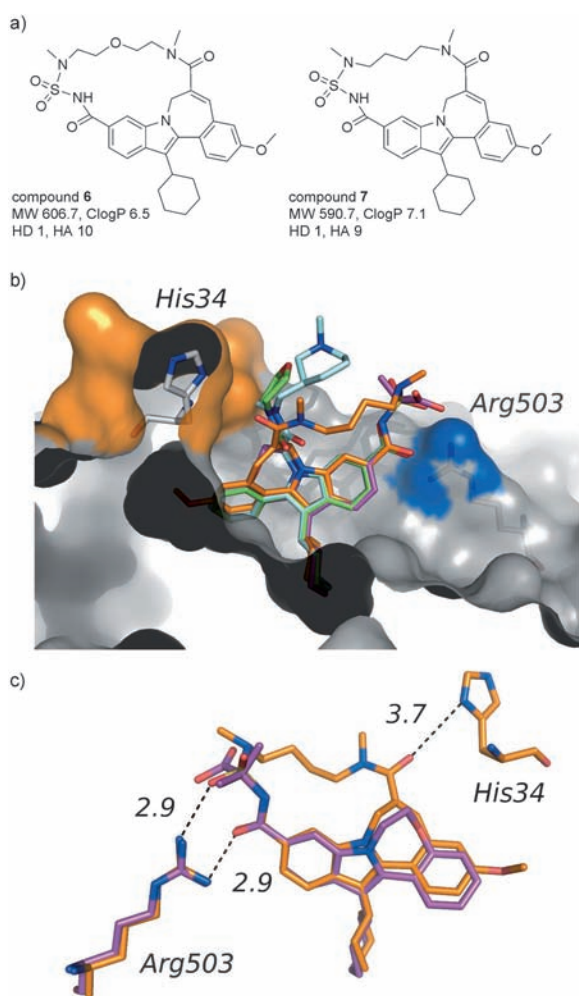


Figure 3. Macrocyclic indole inhibitors. a) Chemical structures of **6** and **7**. b) 2.1 Å resolution crystal structure of **7** (orange color-by-atom; structure deposited as PDB ID 4DRU) bound to genotype 1b HCV NS5B polymerase, with early indole inhibitors overlaid as in Figure 1 a and orange surface indicating the additional residues resolved in the new structure (see text). c) Interaction with Arg503 and His34 for **7** and the indole inhibitor from PDB ID 2DXS (overlay as in Figure 1 a; distances shown in Å).

observed serum shift, we focused on optimization of the [liver]/[serum shifted potency] ratio to maximize in vivo efficacy.

As well as affecting binding affinities and antiviral potencies, macrocyclization yielded inhibitors with improved PK profiles. These compounds show high bioavailability, good liver distribution and moderate clearance, with liver concentrations 7 h post-dose more than 10× greater than the measured serum-shifted potencies in rat (Table 2). Conversely, after extensive optimization efforts most non-macrocyclic compounds were limited by poor bioavailability (e.g. **4**: $F = 10\%$), resulting in poor liver distribution (e.g. **4**: $1.1 \times EC_{50}$ at 50% human serum 6 h post-dose (at 3 mg kg^{-1})).^[8] Although bioavailability could be improved, more optimized non-macrocyclic inhibitors still suffer from poor liver distribution. For example, MK-3281, a compound that entered clinical development, is potent in the replicon with limited

Table 1: In vitro profile of macrocyclic indoles and the acyclic carboxylic acid **4**.

Cmpd.	K_d [nM] ^[a]	k_{off} [s ⁻¹] ^[a]	IC_{50} ^[b] [nM]	EC_{50} ^[c] [nM]	Serum shift ^[d] (-fold)
4	136	380×10^{-5}	48 ^[e]	260	8
6	4.0	10.0×10^{-5}	31	81	9
7	2.4	4.8×10^{-5}	26	75	8

[a] Dissociation constant (K_d) and off-rate constant (k_{off}) determined by surface plasmon resonance with NS5B con1b($\Delta 21$). [b] Inhibition potency on the NS5B $\Delta 21$ polymerase (20 nM). [c] Replicon potency. [d] Ratio of the replicon potency (EC_{50}) measured in the presence of 40% human serum divided by that observed in the absence of human serum. [e] From ref. [25].

serum shift (only 3-fold decrease in EC_{50}) and good bioavailability across different species (49% in rat, 78% in dog), but shows limited liver distribution in rat ($4 \times EC_{50}$ at 50% human serum).^[25] Because it is anticipated that liver distribution and liver/plasma ratio at 7 h post-dose are important contributors to therapeutic efficacy,^[26,27] **6** was selected for clinical development.

Structure-based macrocyclization has led to new inhibitors with improved pre-clinical profiles. We see four key distinctions between the present macrocycles and their non-macrocyclic predecessors. First, the carboxylate of the non-macrocyclic analogues has been replaced by a cyclized acylsulfamide, maintaining specific contact with the guanidine of Arg503 (Figure 3) while eliminating the potential for glucuronidation, a liability for carboxylate-containing drugs. Second, our strategy overcame the requirement for the presence of a basic amine—essential for cellular replicon potency in non-macrocyclic series, and avoids zwitterionic structures—a pharmaceutically undesirable feature.^[7,25] Third, binding of **7** recruits new elements of the inhibitor binding site, providing additional information useful for structure-based design of inhibitors targeted to this site. Fourth, and perhaps most interesting, the macrocyclic inhibitors show improved PK behavior while appearing less “drug-like” than their non-macrocyclic predecessors, according to standard calculated physicochemical criteria of “drug-likeness” (Figure 1–3). Recent analyses indicate that current drug discovery efforts are often focused on molecules at or beyond the frontier of what is generally described as “drug-like” chemical space.^[28–30] This is not, however, entirely unreasonable, since many useful drugs exceed the limits typically implied by the term “drug-like”.^[28,29] Chemistry strategies that facilitate exploration of the limits of what is acceptable chemical space for drugs should lead to improved understanding of the “drug-like” concept, and should allow drug discovery chemists to work with a broader molecular palette. One approach adopted by nature for achieving larger small-molecule bio-actives is the macrocycle;^[1,4] the value of this approach is underscored by the prevalence of macrocycles in bio-active natural products and natural product-derived drugs. Various factors are thought to contribute to the improved drugability of macrocyclic small molecules, including restricted flexibility, reduced metabolism (esp. for cyclized peptides), and shielding of polar atoms through intramolecular hydrogen bonding.^[1,3,4] Rather than being property

Table 2: Pharmacokinetic parameters of macrocyclic analogues **6** and **7** in male Sprague–Dawley rats ($n=3$) and macrocycle **6** in Beagle dogs ($n=3$).^[a]

Species	Cmpd.	$Cl^{[b]}$ [L h ⁻¹ kg ⁻¹]	$t_{max}^{[c]}$ [h]	$C_{max}^{[c]}$ [μM]	$AUC_{inf}^{[c]}$ [μM h]	Liver ^[d] [μM]	L/P ^[e]	L/EC ₅₀ (40% HS) ^[f]	F ^[g] [%]
rat	6	3.2	2.7	0.7	4.8	13.0	46	18	> 66
rat	7	2.4	0.8	1.3	7.0	8.3	23	12	76
dog	6	0.54	1.2	10.2	25.8	–	–	–	87

[a] 2 mg kg⁻¹ intravenous, 10 mg kg⁻¹ peroral; intravenous vehicle PEG400/saline 70/30; peroral vehicle PEG400/2% vitE-TPGS. [b] Plasma clearance.

[c] t_{max} = time to maximum plasma concentration, C_{max} = maximum plasma concentration, AUC_{inf} = area under the curve extrapolated to infinite time.

[d] Liver concentrations after oral administration 7 h post-dosing. [e] Liver/plasma ratio after oral administration 7 h post-dosing. [f] Liver/EC₅₀ (at 40% human serum) ratio. [g] Oral bioavailability.

outliers, these more complex small-molecules may simply be revealing the limitations of standard 2D property calculations. While not unheard of, macrocycles are considered underexploited in current synthetic drugs;^[1] however, recent advances in relevant synthetic chemistry techniques, most notably the pioneering work of Grubbs,^[31,32] have opened the door to broader exploration of synthetic small-molecule macrocycles. In the present work we have used structure-based design to guide macrocyclization, leading to the discovery of new inhibitors that maintain potency while showing substantially improved pharmacokinetic behavior.

Received: January 5, 2012

Revised: February 7, 2012

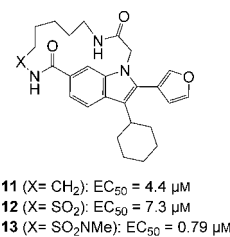
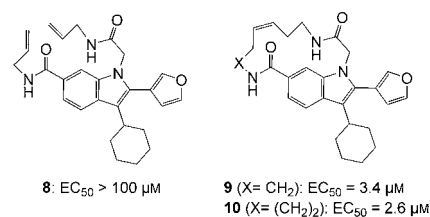
Published online: March 30, 2012

Keywords: hepatitis C virus · inhibitors · macrocycles · polymerases · pharmacokinetics

[17] Y. H. Zhao, M. H. Abraham, J. Le, A. Hersey, C. N. Luscombe, G. Beck, B. Sherborne, I. Cooper, *Pharm. Res.* **2002**, *19*, 1446.

[18] Extensive structure–activity details will be published elsewhere.

[19]



- [1] E. M. Driggers, S. P. Hale, J. Lee, N. K. Terrett, *Nat. Rev. Drug Discovery* **2008**, *7*, 608.
- [2] E. Marsault, M. L. Peterson, *J. Med. Chem.* **1961**, *54*, 1961.
- [3] T. Rezai, J. E. Bock, M. V. Zhou, C. Kalyanaraman, R. S. Lokey, M. P. Jacobson, *J. Am. Chem. Soc.* **2006**, *128*, 14073.
- [4] L. A. Wessjohann, E. Ruijter, D. Garcia-Rivera, W. Brandt, *Mol. Diversity* **2005**, *9*, 171.
- [5] S. Di Marco et al., *J. Biol. Chem.* **2005**, *280*, 29765.
- [6] K. Ikegashira et al., *J. Med. Chem.* **2006**, *49*, 6950.
- [7] I. Stansfield, C. Ercolani, A. Mackay, I. Conte, M. Pompei, U. Koch, N. Gennari, C. Giuliano, M. Rowley, F. Narjes, *Bioorg. Med. Chem. Lett.* **2009**, *19*, 627.
- [8] S. Harper, *J. Med. Chem.* **2005**, *48*, 4547.
- [9] P. L. Beaulieu, J. Gillard, D. Bykowski, C. Brochu, N. Dansereau, J.-S. Duceppe, B. Haché, A. Jakalian, L. Lagacé, S. LaPlante, G. McKercher, E. Moreau, S. Perreault, T. Stammers, L. Thauvette, J. Warrington, G. Kukolj, *Bioorg. Med. Chem. Lett.* **2006**, *16*, 4987.
- [10] I. Stansfield, M. Pompei, I. Conte, C. Ercolani, G. Migliaccio, M. Jairaj, C. Giuliano, M. Rowley, F. Narjes, *Bioorg. Med. Chem. Lett.* **2007**, *17*, 5143.
- [11] J. Habermann, E. Capito, M. del R. R. Ferreira, U. Koch, F. Narjes, *Bioorg. Med. Chem. Lett.* **2009**, *19*, 633.
- [12] M. J. Bailey, R. G. Dickinson, *Chem.-Biol. Interact.* **2003**, *145*, 117.
- [13] M. Castillo, P. C. Smith, *Drug Metab. Dispos.* **1995**, *23*, 566.
- [14] C. Skonberg, J. Olsen, K. G. Madsen, S. H. Hansen, M. P. Grillo, *Expert Opin. Drug Metab. Toxicol.* **2008**, *4*, 425.
- [15] C. Giuliano et al., *Xenobiotica* **2005**, *35*, 1035.
- [16] P. L. Beaulieu et al., *Bioorg. Med. Chem. Lett.* **2010**, *20*, 857.
- [20] ΔC21 form of HCV genotype 1b strain J4 NS5B.
- [21] The inhibitor is bound to one of the two NS5B monomers in the crystallographic asymmetric unit; in the other monomer the fingertip loop displacement required for inhibitor binding is blocked by a crystallographic contact.
- [22] The cyclohexyl ring of the new inhibitor is the most deeply buried part of the bound inhibitor, and the bridged indole-phenyl torsion adopts the dihedral angle observed previously in both free and rigidified systems.^[6]
- [23] B. K. Biswal, M. M. Cherney, M. Wang, L. Chan, C. G. Yannopoulos, D. Bilimoria, O. Nicolas, J. Bedard, M. N. James, *J. Biol. Chem.* **2005**, *280*, 18202.
- [24] 110 min (**6**) and 242 min (**7**), compared to 3 min for the 4–NS5B complex. In some therapeutic contexts increased inhibitor residence time may be of pharmacological benefit.^[33]
- [25] F. Narjes et al., *J. Med. Chem.* **2011**, *54*, 289.
- [26] D. Lamarre et al., *Nature* **2003**, *426*, 186.
- [27] N. J. Liverton et al., *J. Am. Chem. Soc.* **2008**, *130*, 4607.
- [28] A. Alex, D. S. Millan, M. Perez, F. Wakenhut, G. A. Whitlock, *Med. Chem. Commun.* **2011**, *2*, 669.
- [29] P. D. Leeson, B. Springthorpe, *Nat. Rev. Drug Discovery* **2007**, *6*, 881.
- [30] W. P. Walters, J. Green, J. R. Weiss, M. A. Murcko, *J. Med. Chem.* **2011**, *54*, 6405.
- [31] G. C. Vougioukalakis, R. H. Grubbs, *Chem. Rev.* **2010**, *110*, 1746.
- [32] L. Yet, *Chem. Rev.* **2000**, *100*, 2963.
- [33] R. A. Copeland, D. L. Pompliano, T. D. Meek, *Nat. Rev. Drug Discovery* **2006**, *5*, 730.